PAPER

Check for updates

Wetting behavior of zirconia nanotubes†

Swathi Naidu Vakamulla Raghu [iD] and Manuela Sonja Killian [iD] *

In this work, we investigate the wettability of ZrO_2 nanotubes (ZrNT) synthesized *via* electrochemical anodization of zirconium. The ZrNT surface shows super-hydrophilic behavior while the octadecylphosphonic acid ($C_{18}H_{37}PO(OH)_2$) modified surface shows super-hydrophobic behavior. We demonstrate that the wetting properties are independent of ZrO_2 nanotube geometry and length.

Electrochemical anodization is a facile technique used to fabricate highly ordered structures in the sub-micron range. Several metals have successfully demonstrated self-organized porous nanostructure growth under appropriate anodization parameters.[1] Fluoride rich electrolytes contributed a significant advancement to the field, enabling the synthesis of high-aspect ratio nanostructured arrays on 'valve metals' such as zirconium.[2–4] Tuneable surface properties can exploit applications that are surface-interaction dependent, such as *e.g.* catalysis, filtration or coatings.[5–8] Zirconia is a biocompatible, high band-gap material that has reportedly demonstrated superior surface properties for the enhanced attachment of molecules.[9–11] It is used in biomedical devices, sensors and more recently for photocatalytic applications.[12,13] With this intent, ZrNT surfaces are modified by a monolayer of octadecylphosphonic acid rendering it super-hydrophobic.[14] Wang *et al.* previously investigated the pristine ZrNT surface wettability, observing highly hydrophilic properties.[15] In the present study, we synthesize ZrO_2 nanotubular structures in a single step anodization process without the pre-requisite dip-etching process using HF-acid based etchants. This one-pot synthesis allows for less hazardous and safer working conditions. Further, we investigate the influence of nanotube-geometry on the extent of super-hydrophobicity. Zr foils (99.2% purity, Goodfellow UK, 0.125 mm thickness) were ultrasonically cleaned in acetone, methanol and ethanol followed by rinsing in deionized water and dried under a nitrogen stream. Electrochemical anodization was carried out using a high-voltage potentiostat (Jaissle IMP 88-200 PC) in electrochemical cells with a working area of 1 cm² and larger cross-sections were fabricated *via* dip-anodization in an electrochemical bath-type setup. In both cases, a platinum counter electrode was used in a two-electrode setup. Anodization was carried out in a standard glycerol-based electrolyte consisting of 30% formamide, 2 wt% NH_4F (Merck)

and 2 wt% H_2O under various conditions to obtain the respective morphologies. 20 nm wide-tubes were synthesized *via*-dip anodization at 30 V for 25 minutes without ramping and 40 nm wide-tubes, with ramping the potential at 1 V s⁻¹ from OCP and kept at 50 V for 1 h. Thick-walled ~100 nm wide tubes (inner wall '*d*' ~80 nm, wall-thickness '*t*' ~20 nm) were synthesized at 50 V for 30 min without ramping, with the difference of 4 wt% distilled water in the electrolyte. Thin-walled ZrNTs (~100 nm wide, '*t*' ~3 nm) were achieved in 30 min at 90 V (ramp 1 V s⁻¹). The tube length was varied from 3 to 9 μm by adjusting the anodization time. Zr compact oxide (CO) films were prepared on Zr foils under a constant potential of 30 V for 30 min in a 1 M H_2SO_4 (Merck) electrolyte. The anodized samples were rinsed with ethanol and distilled water and dried with nitrogen. To impart surface hydrophobicity, samples were placed in solutions containing 10 mM octadecylphosphonic acid (OPA, $C_{18}H_{37}PO(OH)_2$) in tetrahydrofuran (THF, Roth) for a period of 24 h at ambient conditions, forming self-assembled monolayers (SAMs). Further, the samples were rinsed in pure THF for 30 s and dried under a filtered nitrogen stream. Scanning electron microscopy (Hitachi SEM FE 4800) was employed for the structural and morphological characterization of the anodized zirconia specimens. For chemical characterization, surface modification with OPA was evaluated using a ToF-SIMS IV instrument (ION-TOF, Münster) and coverage was evaluated *via* XPS (Perkin-Elmer Physical Electronics 5600, a detailed experimental description can be found in the ESI†). Static water contact angle (WCA) measurements were performed using both an Ossila-contact angle goniometer and a Leica Suite application instrument (DI water droplet volume, 10 μl) to determine wetting behavior. WCA values from both instruments only deviated within the statistical error of the measurement, as depicted in ESI-Fig. S1.† Fig. 1(a), shows a zirconia substrate with a native oxide film (as received condition), having a hydrophilic WCA of (~30°) owing to surface hydroxyl groups.[16,17] All porous samples depicted here showed super-hydrophilicity due to the improved oxide quality and enhanced liquid impregnation when compared to the native oxide

Chemistry and Structure of Novel Materials, University of Siegen, Paul-Bonatz-Str. 9-11, 57076 Siegen, Germany. E-mail: Manuela.Killian@uni-siegen.de
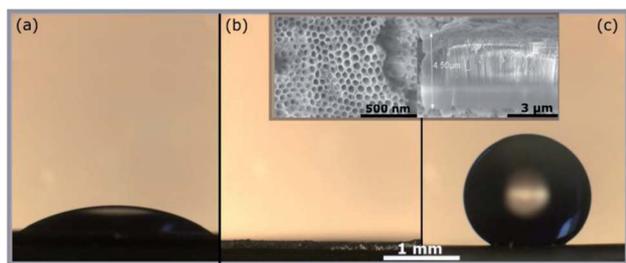
Fig. 1 Optical images of water droplet on ZrO_2 surface. (a) Native oxide (b) bare ZrNTs (c) ZrNTs after attaching OPA SAM. Inset shows SEM top and cross-section of ~100 nm ZrNTs.

Fig. 3 ToF-SIMS spectra of ZrNTs before and after coverage with octadecylphosphonic acid SAMs; (a) Zr^+ isotopic pattern; (b) OPA–H^- molecular signal.

surfaces. The water droplets spread entirely, covering the pores, an example is shown in Fig. 1(b), in agreement to literature.[15]

After surface modification with a monolayer of octadecyl-phosphonic acid, the nanotubes become super-hydrophobic as shown in Fig. 1(c). In Fig. 2, the coverage of ZrO_2 and TiO_2 compact oxides with long chain aliphatic molecules with various functional groups was determined using XPS. OPA showed the highest adhesion to both oxides, followed by octadecyl-trimethoxysilane. Both molecules form denser layers on ZrO_2, as reflected by the enhanced coverage. Stearic acid and octadecylamine yielded significantly lower surface coverages, showing a slightly enhanced adsorption to TiO_2. Phosphonic acid-based SAMs consequently offer the highest potential for the formation of superhydrophobic coatings on both ZrO_2 and TiO_2 among the investigated functional groups.

ToF-SIMS measurements were performed to evaluate the OPA-attachment and the resulting spectra in Fig. 3 confirms the presence of the phosphonic acid on ZrNT *via* the detection of the characteristic quasi-molecular signal of OPA ($m/z = 333.29$, $C_{18}H_{38}PO_3^-$, M–H^-) in accordance to reported literature.[11,18,19] Fig. 4(a) depicts the morphology of ZrNT ($d \leq 20$ nm) and the WCA ($162° \pm 1°$).

This is currently the smallest reported ZrNT diameter achieved *via* a single-step anodization. When functionalized with a SAM, it reports a superhydrophobic WCA. Moreover, in Fig. 4
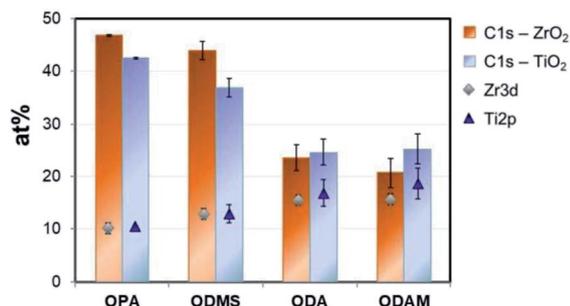
the WCAs on zirconia test surfaces with larger pore configurations: 'd' nm ~40, ~100 nm-thick and thin-walled NTs and CO, (b–d) reveal that changing the porosity (difference in surface area made up of the solid), did not affect the extent of

Fig. 4 Optical images of water droplets on SAM modified ZrNT structures of different porosity and corresponding SEM images (scale bar – 500 nm) of the surfaces. Diameters, (a) $d \leq 20$ nm, (b) $d = 40$ nm, (c) thick walled $d = 100$ nm, (d) thin walled $d = 100$ nm and (e) compact anodic oxide (droplet image – scale bar = 1 mm).

Fig. 2 Adsorption (atomic percentage (at%)) of organic molecules to ZrO_2 (C 1s–ZrO_2 signal) and TiO_2 (C 1s–TiO_2 signal) and substrate signals respectively (Zr 3d and Ti 2p) measured using XPS for 18-C carbohydrate molecules with different anchoring groups (OPA – octadecylphosphonic acid, ODMS – octadecyltrimethoxysilane, ODA – stearic acid, ODAM – octadecylamine).
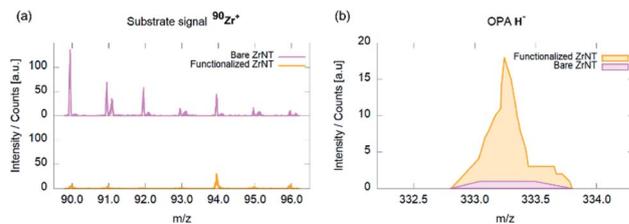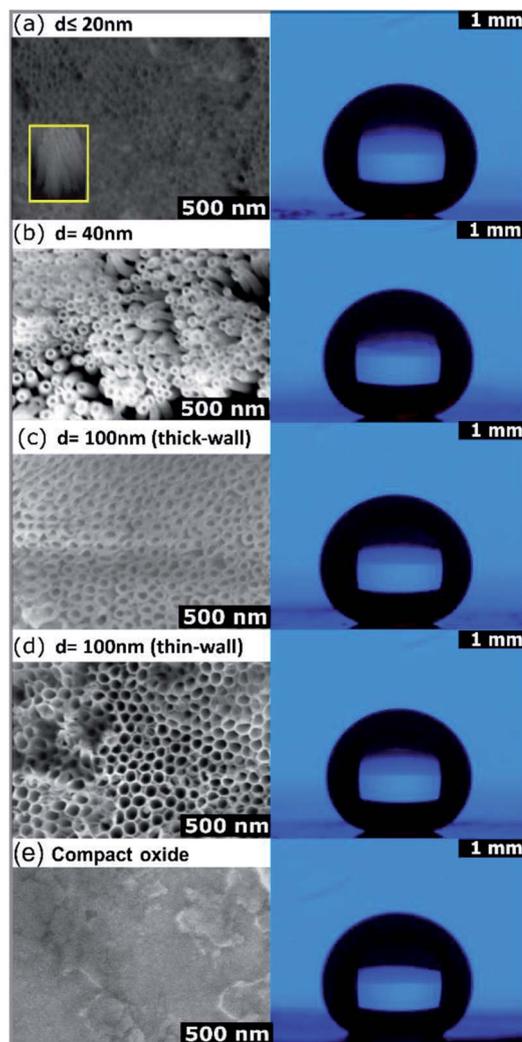
Paper

hydrophobicity, thereby maintaining a nearly constant WCA of $(160° \pm 1°)$ on the respective nanotubular surfaces. The only difference appeared when comparing ZrNTs to a ZrCO surface, for which a WCA of 120° (Fig. 4(e)) was recorded. It may be noted that the Zr-substrates have poor conductivity resulting in challenges such as excessive charging and lower focusing abilities while performing SEM characterization. Images shown in Fig. 4 have uniform scale-bars (SEM – 500 nm and WCA – 1 mm). Table 1 summarizes the influence of these pore geometries on WCAs.

In Fig. 5, WCA measurements were performed on OPA modified ZrNT of varying lengths to evaluate the influence of tube length on the wettability, yielding no statistical changes in dependence of tube length. A uniform nanoporous array is a homogenous surface with an increased roughness factor when compared to a 'flat' surface and hence in Fig. 1(a and b), the transition from hydrophilic to super-hydrophilic state is well accommodated by the Wenzel approach.[20] This phenomenon is represented as an enhanced wetting process that occurs as a result of liquid–solid interaction in the absence of air resistance. After successful surface modification with OPA (Fig. 1(c)), the methyl-terminated SAM surface is strongly water-repellent. This results in some cases where the water droplets continue to bounce of the surface and if they do adhere, they form high WCAs ($\geq 150°$). The super-hydrophobic state is stabilized and explained by the Cassie–Baxter model (CBM) as a result of a greater interaction with trapped air in-between the liquid–solid layers.[21] As represented in Fig. 4(a–d), the average WCAs measured were ($\sim 160°$) for the ZrNT surfaces. The WCA values (θ^*) can be expressed according to the Cassie–Baxter equation, wherein (θ) is the WCA measured on the SAM modified flat zirconia surface, 'f' is a morphological factor and is defined as the area fraction of solid–liquid contact and ($1 - f$) is the area fraction of air–liquid interface.

$$\cos(\theta^*) = f^* \cos(\theta) - (1 - f) \tag{1}$$

These surface fractions were calculated from high resolution SEM images as represented in Fig. 4, by estimating the ratio between pore walls to the total area respectively and complemented with ImageJ analysis. The morphological factor 'f'
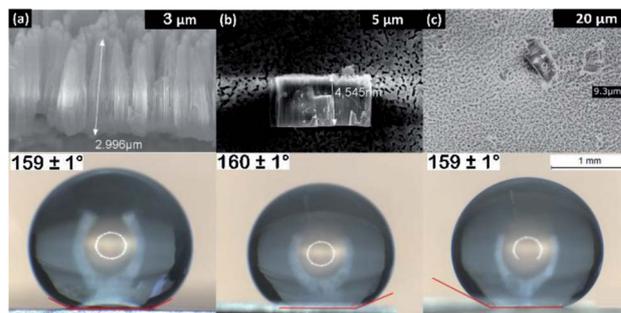

Fig. 5 Optical images of water droplets on SAM modified ZrNT structures of different oxide-layer thickness and corresponding SEM images of the cross-sections. Length (a) ~ 3 µm, (b) ~ 4.5 µm and (c) ~ 9 µm.

for values represented in Table 1 was calculated to be 0.020, 0.047, 0.131, 0.052 for ('d' nm = 20, 40, 100 – thick-walled and thin-walled) ZrNTs, respectively. Recently, it was reported that the wettability of titania nanotubes is dependent of tube diameter and the observations were perfectly supported by eqn (1) as proposed by the CBM.[22] For this result to hold true in the case of zirconia, the dimensionless factor 'f' in eqn (1) is represented as the ratio between the 'projected area' to the 'total area' where, the projected area 'P' is

$$P = 2\pi r \varepsilon \tag{2}$$

where, 'ε' denotes the wall thickness, while 'r' is the radius of the pore. The newly calculated morphological factor 'f' using eqn (2) for values represented in Table 1 was calculated to be 0.015, 0.048, 0.079, 0.066 for ('d' nm = 20, 40, 100 – thick-walled and thin-walled) ZrNTs, respectively, indicating that the thin-walled NTs are more densely packed than the thick walled. Theoretical values continue to be greater than experimentally measured WCAs for all three morphologies. The experimental values are identical on all substrates, averaging at a value of ($\sim 160°$). This value is at the physical limit of experimental measurements for low-energy surfaces and, hence, acts as a limiting criterion while quantifying the 'extent' of an already super-hydrophobic surface.[22] This essentially means that the surfaces measured experimentally may indeed have higher WCA values that are in reality closer to the theoretical calculations. Additionally, the proposed modification to the CBM due to incorporation of the wall-thickness accounts for the super-hydrophobic phenomenon exhibited by ZrNTs irrespective of pore-diameter, because the 'f' factor is comparable due to the type of packing exhibited by all three substrates. Implying that for a droplet of fixed volume, the drop-contact line interacts with similar solid fractions. Thus, superhydrophobicity observed for ZrNTs even at smaller pore-diameters is consistent with the constant WCAs reported for titania (increasing diameters will increase surface hydrophobicity).[22] Nevertheless, the droplet always remains balanced in CBM.[20,21] There appear a few variations in theory and experimental and may be attributed to the physical limits of experimental measurement as described earlier. In comparison to previous reports by Wang *et al.*,[14] this

Table 1 Influence of pore-diameter on WCAs, measured and calculated values (according to Cassie–Baxter model and the proposed modification (ε) to it)

Pore diameter (nm)	Water contact angle (°)		
	Experimental	Cassie – Baxter model	
		Theoretical	Modified-theoretical
~ 20	162 ± 1	172	173
~ 40	159 ± 1	168	167
Thick-wall (~ 100)	160 ± 1	159	164
Thin-wall (~ 100)	160 ± 1	167	165
Compact oxide	120 ± 2	—	—

is the first reported observation of superhydrophobic WCA on functionalized ZrNT for ($d \leq 20$ nm) produced *via* a single-step anodization. Additionally, the WCA of ZrNTs is also independent of length.

In conclusion, the nanoporous ZrO_2 layers produced *via* anodization show a transition from super-hydrophilic to super-hydrophobic surfaces when modified with a (non-fluorinated) octadecylphosphonic acid monolayer. Within the investigated range, WCAs remain constantly super-hydrophobic ($\sim160°$), irrespective of the change in pore diameters and length, thereby following the Cassie–Baxter model. By including the influence of a geometric parameter accommodating the wall thickness, the roughness factor is balanced and continues to remain within the transition threshold of the super-hydrophobic state. Such an observation is of importance as it offers insights into material behavior and is responsible for enhanced degrees of freedom during the fabrication process, such that both simple and complex geometries may still be able to elicit identical surface response. This level of flexibility offers the possibility to work with wider operating parameters involving the anodization process.

Author contributions

SNVR – conceptualization, data curation, methodology, investigation, writing – original draft. MSK – funding acquisition, project administration, supervision, resources and review & editing.

Conflicts of interest

There are no conflicts to declare.

Acknowledgements

Notes and references

1 M. Kulkarni, A. Mazare, P. Schmuki and A. Iglic, Influence of Anodization Parameters on Morphology of TiO_2 Nanostructured Surfaces, *Adv. Mater. Lett.*, 2016, **7**(1), 23–28, DOI: 10.5185/amlett.2016.6156.

2 H. Tsuchiya, J. M. Macak, I. Sieber and P. Schmuki, Self-Organized High-Aspect-Ratio Nanoporous Zirconium Oxides Prepared by Electrochemical Anodization, *Small*, 2005, **1**(7), 722–725, DOI: 10.1002/smll.200400163.

3 A. W. Amer, S. M. Mohamed, A. M. Hafez, S. Y. Alqaradawi, A. S. Aljaber and N. K. Allam, Self-Assembled Zirconia Nanotube Arrays: Fabrication Mechanism, Energy Consideration and Optical Activity, *RSC Adv.*, 2014, **4**, 36336–36343, DOI: 10.1039/c4ra05115g.

4 J. M. Macak, L. V. Taveira, H. Tsuchiya, K. Sirotna, J. Macak and P. Schmuki, Influence of Different Fluoride Containing Electrolytes on the Formation of Self-Organized Titania Nanotubes by Ti Anodization, *J. Electroceram.*, 2006, **16**, 29–34, DOI: 10.1007/s10832-006-3904-0.

5 V. Grover, R. Shukla and A. K. Tyagi, Facile Synthesis of ZrO_2 Powders: Control of Morphology, *Scr. Mater.*, 2007, **57**(8), 699–702, DOI: 10.1016/j.scriptamat.2007.06.053.

6 A. G. Sanchez, W. Schreiner, G. Duffó and S. Ceré, Surface Characterization of Anodized Zirconium for Biomedical Applications, *Appl. Surf. Sci.*, 2011, **257**(15), 6397–6405, DOI: 10.1016/j.apsusc.2011.02.005.

7 W. Li, H. Huang, H. Li, W. Zhang and H. Liu, Facile Synthesis of Pure Monoclinic and Tetragonal Zirconia Nanoparticles and Their Phase Effects on the Behavior of Supported Molybdena Catalysts for Methanol-Selective Oxidation, *Langmuir*, 2008, **24**(15), 8358–8366, DOI: 10.1021/la800370r.

8 S. N. V. Raghu, H. Chuluunbandi and M. S. Killian, Zirconia nanotube coatings - UV-resistant superhydrophobic surfaces, *Surf. Interfaces*, 2021, **26**, 101357, DOI: 10.1016/j.surfin.2021.101357.

9 J. C. Garcia, L. M. R. Scolfaro, A. T. Lino, V. N. Freire, G. A. Farias, C. C. Silva, H. W. L. Alves, S. C. P. Rodrigues and E. F. Da Silva, Structural, Electronic, and Optical Properties of ZrO_2 from *Ab Initio* Calculations, *J. Appl. Phys.*, 2006, **100**, 104103, DOI: 10.1063/1.2386967.

10 S. Heiroth, R. Ghisleni, T. Lippert, J. Michler and A. Wokaun, Optical and Mechanical Properties of Amorphous and Crystalline Yttria-Stabilized Zirconia Thin Films Prepared by Pulsed Laser Deposition, *Acta Mater.*, 2011, **59**(6), 2330–2340, DOI: 10.1016/j.actamat.2010.12.029.

11 M. S. Killian, *Organic Modification of TiO_2 and Other Metal Oxides with SAMs and Proteins - a Surface Analytical Investigation*, PhD Dissertation, Friedrich-Alexander, University Erlangen-Nuremberg, 2013.

12 C. Piconi and G. Maccauro, Zirconia as a Ceramic Biomaterial, *Biomaterials*, 1999, **21**(1), 1–25, DOI: 10.1016/S0142-9612(98)00010-6.

13 Q. Yuan, Y. Liu, L. L. Li, Z. X. Li, C. J. Fang, W. T. Duan, X. G. Li and C. H. Yan, Highly Ordered Mesoporous Titania-Zirconia Photocatalyst for Applications in Degradation of Rhodamine-B and Hydrogen Evolution, *Microporous Mesoporous Mater.*, 2009, **124**(1–3), 169–178, DOI: 10.1016/j.micromeso.2009.05.006.

14 W. Gao, L. Dickinson, C. Grozinger, F. G. Morin and L. Reven, Self-Assembled Monolayers of Alkylphosphonic Acids on Metal Oxides, *Langmuir*, 1996, **12**(26), 6429–6435, DOI: 10.1021/la9607621.

15 L.-N. Wang, C. Shen, A. Shinbine and J.-L. Luo, Variation on Wettability of Anodic Zirconium Oxide nanotube surface, *Thin Solid Films*, 2013, DOI: 10.1016/jtsf.2013.01.066.

16 R. Wang, K. Hashimoto, A. Fujishima, M. Chikuni, E. Kojima, A. Kitamura, M. Shimohigoshi and T. Watanabe, Light-Induced Amphiphilic Surfaces [4], *Nature*, 1997, **388**, 431–432, DOI: 10.1038/41233.

17 H. Tamura, K. Mita, A. Tanaka and M. Ito, Mechanism of Hydroxylation of Metal Oxide Surfaces, *J. Colloid Interface Sci.*, 2001, **243**(1), 202–207, DOI: 10.1006/jcis.2001.7864.

18 M. S. Killian, J. F. Gnichwitz, A. Hirsch, P. Schmuki and J. Kunze, ToF-SIMS and XPS Studies of the Adsorption Characteristics of a Zn-Porphyrin on TiO$_2$, *Langmuir*, 2010, **26**(5), 3531–3538, DOI: 10.1021/la9032139.

19 H. Y. Nie, Revealing Different Bonding Modes of Self-Assembled Octadecylphosphonic Acid Monolayers on Oxides by Time-of-Flight Secondary Ion Mass Spectrometry: Silicon *vs.* Aluminum, *Anal. Chem.*, 2010, **82**(8), 3371–3376, DOI: 10.1021/ac100671q.

20 R. N. Wenzel, Resistance of Solid Surfaces to Wetting by Water, *Ind. Eng. Chem.*, 1936, **28**(8), 988–994, DOI: 10.1021/ie50320a024.

21 A. B. D. Cassie and S. Baxter, Wettability of Porous Surfaces, *Trans. Faraday Soc.*, 1944, **40**, 546–551, DOI: 10.1039/tf9444000546.

22 E. Balaur, J. M. Macak, H. Tsuchiya and P. Schmuki, Wetting Behaviour of Layers of TiO$_2$ Nanotubes with Different Diameters, *J. Mater. Chem.*, 2005, **15**(42), 4488–4491, DOI: 10.1039/b509672c.